

Synthesis, Structure, Magnetic Properties and Aqueous Optical Citrate Detection of Chiral Dinuclear Cu^{II} Complexes

Snehadrinarayan Khatua,^[a] Kibong Kim,^[a] Jina Kang,^[a] Jung Oh Huh,^[b]
Chang Seop Hong,^[c] and David G. Churchill^{*[a]}

Keywords: Chiral dicopper complex / Schiff bases / Magnetic properties / Structure elucidation / Citrate detection

Two chiral dimeric Cu^{II} Schiff base complexes, Na₂[Cu(S-lys)₂·(H₂O)₂·(ClO₄)₂] (1) and [Cu(S-ornH)₂·(H₂O)₂·(ClO₄)₂] (2) have been prepared by an easy one-pot method in which the L-lysine and L-ornithine-based Schiff base ligands are generated in situ. These complexes have been characterized by various spectroscopic techniques and single-crystal X-ray diffraction. The molecular structures show that both complexes are indeed dimeric with Cu^{II} centers that are phenolate-bridged. Variable-temperature magnetic analysis revealed that a strong antiferromagnetic coupling interaction

was mediated through the phenolate bridge between the two Cu^{II} centers. Since these compounds were highly soluble in water, we explored carboxylate sensing capability through colorimetric indicator displacement assays (IDAs). By using pyrocatechol violet (PV) as a displaceable colorimetric indicator, citrate ion selectivity was demonstrated in 100 % water solution in the physiological pH range.

(© Wiley-VCH Verlag GmbH & Co. KGaA, 69451 Weinheim, Germany, 2009)

Introduction

Extensive and continued interest exists in the coordination chemistry of transition metals with Schiff base ligands containing strong donor groups like the phenoxyl oxygen atom and imine nitrogen atoms due to the wide range of applications and structural aspects of the resulting transition metal complexes.^[1] The growing number of mono- and di-nuclear copper(II) complexes of Schiff base ligands have led to a more complete understanding of magnetochemistry^[2] in these systems and also of their potential key roles in many biological applications such as antibacterial, antiviral, antifungal species and DNA cleaving agents.^[3] Chiral copper complexes have been used in types of asymmetric catalysis such as olefin polymerization/enantioselective epoxidation, asymmetric hetero-Diels Alder reactions, etc.^[4] as well as in molecular and ion sensing.^[4f] One simple approach for the generation of new *chiral* metal complexes is the use of an amino acid as the chiral source. While there

are some reports relating to such copper(II) amino-acid-based Schiff base complexes, or their reduced versions, the context of study in these reports has been on metallo-supramolecular architecture formation.^[5]

Such *di*-copper design bearing proximal centers also allows for the possibility of selective binding and potential detection of biological analytes, such as anions (i.e., carboxylates and phosphates). Such exciting possibilities of preparing and applying new recognition systems in further understanding of important and/or new biological processes are interesting to many chemical researchers.^[6–7] In particular, citrate is a key species in many biological processes: e.g., the Krebs cycle for cellular respiration. Also, it is used in fatty acid synthesis, photorespiration, glyoxylate cycle and nitrogen metabolism.^[8] The concentration of citrate in urine may signal renal distress or pathology.^[9] Many molecular sensors for detecting citrate have been developed including ones that involve organic molecules, metal complexes, and supramolecular systems.^[10] Also, selective sensors for other carboxylates such as oxalate, malonate, succinate, glutarate, adipate have been reported.^[11]

There are several reports of Schiff base ligand as chemosensors for cation and anions^[12] and copper complexes for anion sensing^[13] but no such report of a copper(II) Schiff base complex that serves as an acid anion sensor in water at physiological pH. Recently we reported the (i) fluorometric and colorimetric (IDA) sensing of phosphate anion in water at physiological pH and (ii) the Cu²⁺ detection by displacement approach, both by an analogous dizinc complex.^[14] This system was highly selective in both cases. In this paper, we will present and discuss the synthesis of water

[a] Molecular Logic Gate Laboratory, Department of Chemistry, Korea Advanced Institute of Science and Technology (KAIST), 373-1 Guseong-dong, Yuseong-gu, Daejeon, 305-701, Republic of South Korea
Fax: +82-42-350-2810
E-mail: dchurchill@kaist.ac.kr

[b] Molecular Materials Laboratory, Department of Chemistry, Korea Advanced Institute of Science and Technology (KAIST), 373-1 Guseong-dong, Yuseong-gu, Daejeon, 305-701, Republic of South Korea

[c] Department of Chemistry and Centre for Electro- and Photo-Responsive Molecules, Korea University, Seoul, 136-701, Republic of South Korea

Supporting information for this article is available on the WWW under <http://dx.doi.org/10.1002/ejic.200900357>.

soluble Cu^{II} complexes Na₂[Cu(*S*-lys)₂·(H₂O)₂](ClO₄)₂ (**1**) and [Cu(*S*-ornH)₂·(H₂O)₂](ClO₄)₂ (**2**) by an easy “one-pot” method, and their capacity to selectively sense citrate in water. The structural, variable-temperature magnetic susceptibility results and chiral properties of these compounds will also be discussed herein.

Results and Discussion

Synthesis and Characterization of Chiral Dimeric Cu^{II} Schiff Base Complexes

Dinuclear copper complexes of *L*-lysine/*L*-ornithine-based Schiff base ligands (Scheme 1) were synthesized by a “one-pot” method. The Schiff base ligands are formed in situ (Scheme 1). The synthetic Scheme is analogous to that of the dinuclear zinc complexes recently reported by our research group.^[14] The aqueous solution of copper perchlorate^[14c] was added to the salicylaldehyde in ethanol, followed by the addition of aqueous solution of *L*-lysine/*L*-ornithine. An aqueous NaOH solution was then added dropwise into the reaction mixture; finally a few drops of triethylamine were added to the reaction mixture to maintain a pH value of ca. 7.0. The formation of a dark greenish colour indicated the formation of the final product. Evaporation gave a green crystalline material, portions of which were characterized by elemental analyses, IR, UV/Vis, ESI-MS, CD spectroscopy, and finally by single-crystal X-ray diffraction.

Solution Behaviour of Chiral Dimeric Cu²⁺ Compounds

The solution properties of complexes **1** and **2** were studied by UV/Vis, circular dichroism (CD) and ESI-MS spectroscopy. Due to the paramagnetic nature of the Cu²⁺ complex, we did not attempt NMR spectroscopic characterization here; the Zn²⁺ analogues were, however, characterized previously by various NMR spectroscopic experiments.^[14]

The UV/Vis spectrum of compounds **1** and **2** were recorded in aqueous buffer solution (pH 7.4, 0.01 M HEPES) at room temperature which shows intense peaks at 356 nm and 266 nm assigned to the LMCT and *intra*-ligand charge transfer transitions, respectively. The broad *d-d* transition was also assigned (600–800 nm) in concentrated (100 mM) solution (Figure S1 and S2, Supporting Information).

The ESI-MS spectra of compounds **1** and **2** were collected in a water/methanol mixture. The spectra of these compounds clearly show a 100% positive ion peak at 623.10 and 595.06 (Figure S3 and S4, Supporting Information). This result suggests that both complexes are stable as dimers in solution over the course of days.

Both compounds are chiral due to the incorporation of *L*-lysine and *L*-ornithine residues as part of the Schiff base ligand. The solution CD spectra of compounds **1** and **2** were collected in a buffered aqueous solution (pH 7.4, 0.01 M HEPES) at 25 °C. The spectra of both compounds are very similar and reveal negative Cotton effects at ca. 362 and ca. 276 nm, respectively (Figure 1).

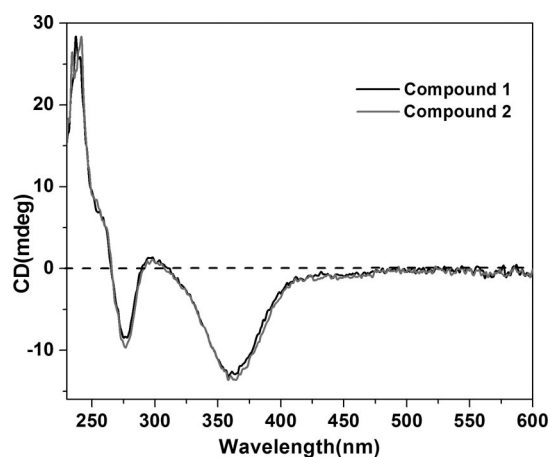
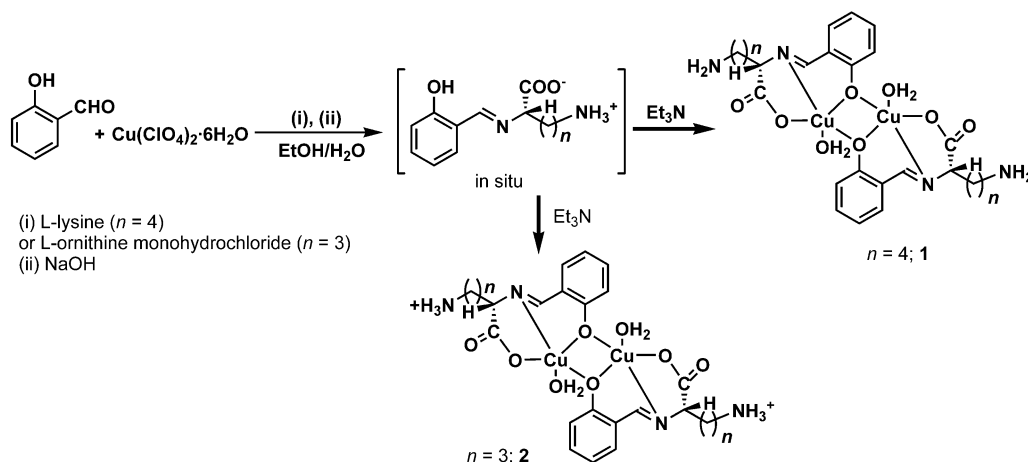


Figure 1. Aqueous circular dichroism (CD) spectra of compounds **1** and **2** (pH 7.4, 0.01 M HEPES, cell path length: 1 cm).



Scheme 1. Synthesis of dimeric Cu²⁺ compounds **1** and **2**.

X-ray Crystallography

Single-crystal X-ray diffraction analysis revealed that complexes **1** and **2** crystallize in the chiral monoclinic space group $C2$. The molecular structures of these compounds are shown in Figures 2 and 3, respectively.

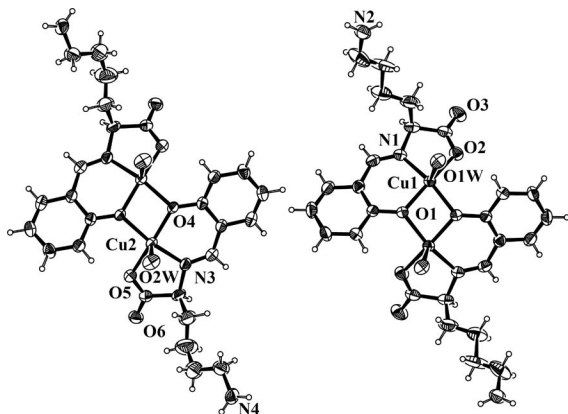


Figure 2. Crystal structure of the compound $\text{Na}_2[\text{Cu}(\text{S-lys})_2 \cdot (\text{H}_2\text{O})_2] \cdot (\text{ClO}_4)_2$ (**1**). Thermal ellipsoids are drawn at 30% probability level. Two sodium and two disordered perchlorate anions are removed for clarity.

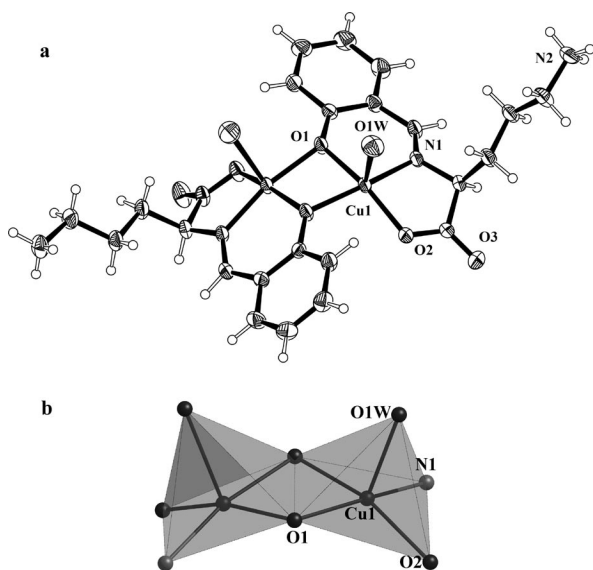


Figure 3. (Top, a) Crystal structure of the compound $[\text{Cu}(\text{S-ornH})_2 \cdot (\text{H}_2\text{O})_2] \cdot (\text{ClO}_4)_2$ (**2**). Thermal ellipsoids are drawn at 30% probability level. Perchlorate anions were crystallographically disordered and are omitted for clarity. (Bottom, b) Core structure of compound **2**.

Structure of $\text{Na}_2[\text{Cu}(\text{S-lys})_2 \cdot (\text{H}_2\text{O})_2] \cdot (\text{ClO}_4)_2$ (1**):** The unit cell of compound **1** clearly contains two crystallographically independent dimeric copper complex units. In each of the dimeric complexes, both Cu^{2+} centers adopt a distorted square pyramidal geometry by coordinating two tridentate L-lysine-based Schiff base ligands. The out-of-plane ($\text{O1-N2-N1-O1}^\#$) distances for the copper centers are 0.23 and 0.21 Å for the two independent complexes. The phenolate oxygen atoms are bridging the two copper centers. Two axial water molecules are directed out from the

same side of the dimer (vide infra). The complex is neutral; but, Na^+ and ClO_4^- counterions are present in the unit cell which probably assist in the adequate crystallinity of this compound. This compound forms 3D networks in the solid state due to a hydrogen bonding interaction which involves the perchlorate oxygen, axial *aqua* ligands and hydrogens of the amine side-chain (Figure 4, a).

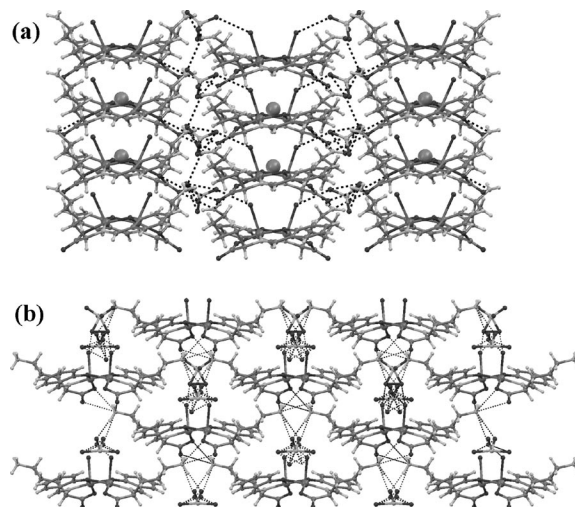


Figure 4. (a) Hydrogen-bonded 3D packing structures for compound **1** and (b) compound **2** (dotted lines represent hydrogen bonding).

Structure of $[\text{Cu}(\text{S-ornH})_2 \cdot (\text{H}_2\text{O})_2] \cdot (\text{ClO}_4)_2$ (2**):** The crystal structure of this complex is approximately the same as that of compound **1**. The coordination environment around the Cu^{2+} center is the same as that for **1**, with only minor differences in bond lengths and angles (Figure 3). In the unit cell there is a single independent dimeric copper complex (**2**) present. This molecule is formulated with charged terminal $-\text{NH}_3^+$ groups, countered by two perchlorate ions, both found to be crystallographically disordered (and modelled accordingly). Also in **2**, both copper centres adopt a distorted square pyramidal geometry in which the out-of-plane distance is 0.23 Å. A packing diagram reveals hydrogen bonded 3D network as a prominent intermolecular interaction in the solid state (Figure 4, b).

The molecular structures of compounds **1** and **2** are quite uncommon, in which the two square-pyramidal coordination polyhedra share an edge, and in which the axial solvato ligands are present on the same side (C_2 -symmetric molecule). It is noteworthy that when D/L lysine was used, a dimeric copper nitrate complex of D/L-lysine Schiff base ligand was formed. This led to two axial ligands present on opposite sides ("up-down" axial ligation) giving a C_i -symmetric molecule. The "up-down" axial ligation obviously arises from a racemic compound in which one amino acid moiety on one end of the molecule is derived from D-Lysine and the other moiety on the other end is L-Lysine (D. G. Churchill, Molecular Logic Gate Lab, unpublished data). A CSD search (CSD version 5.30) yields only few closely related copper dimers; the Research of J. J. Vittal (National University of Singapore) is of particular note regarding

these types of complexes. These involve reduced Schiff base ligands that bear close structural similarity;^[15] there are no such previous reports of copper dimers with Schiff base ligands.

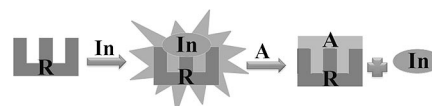
Magnetic Properties

The magnetic susceptibility for **1** and **2** and the temperature dependence thereof has been determined and are presented here. Data was collected at 1 T for the temperature range from 2–300 K (Figure 5). The values of $\chi_m T$ at 300 K are 0.35 and 0.33 cm³ K mol⁻¹, which are significantly smaller than that expected from two noncoupled Cu²⁺ spins. As the temperature is lowered, the $\chi_m T$ product undergoes a dramatic decrease, indicating the presence of strong antiferromagnetic interactions. To probe the magnetic exchange coupling between magnetic centers through the phenoxyl bridges, we employed a dimer model using the spin Hamiltonian $H = -JS_1 \cdot S_2$. The intermolecular magnetic interactions (θ) and a trace amount of paramagnetic impurity (ρ) were also taken into account. A best fit gave $g = 2.0$, $J = -317$ cm⁻¹, $\theta = -18$ K, $\rho = 0.036$ for **1**, and $g = 2.0$, $J = -487$ cm⁻¹, $\theta = -74$ K, and $\rho = 0.055$ for **2**. These results clearly demonstrate the operation of strong intradimer antiferromagnetic couplings, mediated by the phenoxide linkage in which the obtained J values are close to those of Cu²⁺ dimers possessing square pyramidal geometries about both metal centers.^[16]

On the basis of the average Cu–O–Cu angles ($a_{avg} = 98.5^\circ$) for **1** and **2**, the magnetic traits are consistent with predicted values for hydroxy-bridged Cu²⁺ binuclear systems in which an antiferromagnetic nature emerges with $a > 97.5^\circ$.^[17] Stronger intradimer interactions are evident in the case of **2** over that of **1**, which may be associated with a subtle difference in relevant structural parameters: while the mean Cu–O–Cu angles (a_{avg}) and Cu–O lengths (1.96 Å) for both complexes are virtually the same, the dihedral angles between the two [N₂O₂] basal planes are slightly different (41° for **2** and 42° for **1**). The enhanced structural distortion in **1** may give rise to a reduction of the overlap between the magnetic $d_{x^2-y^2}$ orbitals of the adjacent Cu²⁺ centers, eventually leading to the observed decrease in magnetic strength. The interdimer interactions in **2** are stronger than those in **1**, due perhaps to the fact that perchlorate anions in **2** form a close contact with Cu²⁺ ions; in contrast, chloride ions in **1** remain far away from the magnetic centers.

Gauging Anion Sensing Capability

Novel chromo-/fluorogenic systems may provide opportunities for the development of practical, small-molecular systems that involve rapid optical responses upon interactions between receptor and analyte (vide infra).^[18] In recent years, indicator displacement assays (IDAs) or a chemosensing ensemble (CE) approach is a very popular and well-accepted method for sensing which requires a non-chromogenic and non-fluorescent receptor (Scheme 2).^[19] This indirect (IDA) method of detection is a facile route in producing clear optical changes during detection of target analytes which we describe for compounds **1** and **2** below.



Scheme 2. A generalized representation of the indicator displacement assay (IDA) in which an indicator (In) is displaced by the analyte (A) in question. In this work, A is citrate.

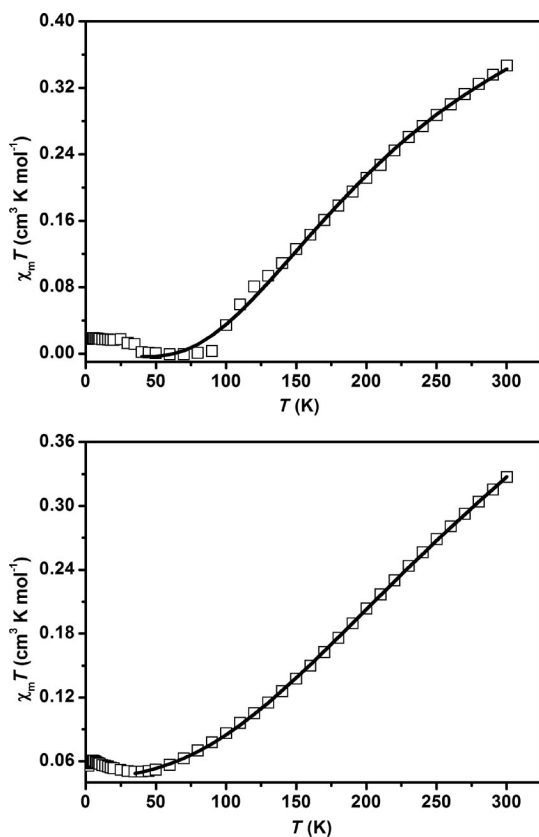


Figure 5. Plot of $\chi_m T$ vs. T for compound **1** (top) and compound **2** (bottom). The solid lines represent the best fitting of the data.

The aqueous solutions of two dinuclear copper complexes **1** and **2** are optically green and nonfluorescent. So, fluorescent detection of anions was not possible by way of these complexes. We instead pursued colorimetric detection of anions, but no selectivity was observed. To determine the potential sensing behaviour of these Cu²⁺ complexes towards di- and tri-carboxylate species, various colorimetric and fluorometric indicators were tested according to the (IDA) protocol. Pyrocatechol violet (PV) showed the best response for the dye molecules tested (see Electronic Supporting Information). PV is a colorimetric indicator known to bind phenolate-bridged bimetallic complexes.^[19c,19f] For this indicator displacement approach, an aqueous buffer solution of PV was used in titrating complexes **1** and **2** and monitored through the change in the UV/Vis spectra. A

gradual decrease of the initial absorption band of PV at 437 nm was accompanied by a concomitant increase in a band centered at 601 nm (**1**). A similar spectrum was observed for compound **2** in which the PV band gradually decreased to give an increase at 597 nm. Separate Job plots confirmed a 1:1 binding stoichiometry of PV to compounds **1** and **2** (see Supporting Information). A curve-fitting analysis produced the experimental association constants: $K_a = 2.45 \pm 0.20 \times 10^2 \text{ M}^{-1}$ for **1**, and $6.14 \pm 0.21 \times 10^2 \text{ M}^{-1}$ for **2** (Figure 6).

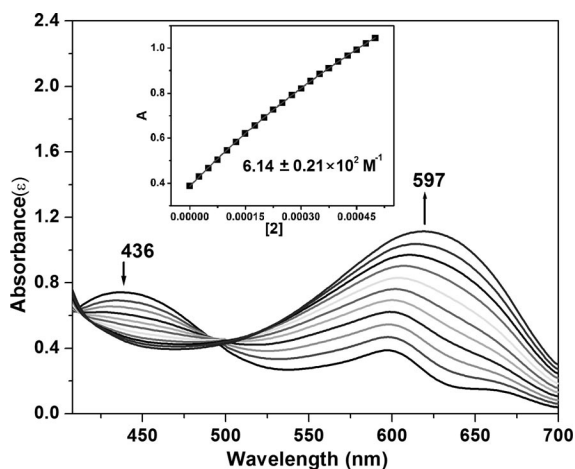


Figure 6. UV/Vis spectrum obtained by addition of solution of **2** (500 μM) to an aqueous buffer solution containing PV (50 μM) (10 mM HEPES, pH 7.4). (Inset) Curve fitting of absorbance change vs. [complex **2**] at 597 nm.

To determine the capacity of selective anion detection of complexes **1** and **2**, various anions (citrate, oxalate, malonate, glutarate, succinate, and adipate) were tested with a 1:1 ensemble of PV and complex **2** (see Supporting Information for binding capabilities for compound **1**). The absorption spectra for the 1:1 mixtures of PV complex **2** along with 5 equiv. of various anions are shown in Figure 7. For all the anions tested here, only citrate was able to restore the colour of PV and give spectral features that relate to liberated PV. The band at 597 nm gradually decreased, whereas the band at ca. 434 nm increased. A clear isosbestic point at 497 nm implies that only two species (PV·**2** and the **2**-citrate conjugate) are present and related by a direct equilibrium. Relatively smaller changes were observed when the PV·**2** ensemble was titrated with oxalate. The Job plot confirms a 1:1 binding stoichiometry between the PV·**2** 1:1 mixture and the citrate analyte.

The association constant for citrate-di-copper complex binding was obtained by a non-linear curve fitting of the PV·**2** ensemble and citrate requiring the UV/Vis titration data (Figure 8).^[20] An association constant (K_a) is $1.99 \pm 0.34 \times 10^4 \text{ M}^{-1}$ was obtained which is significantly bigger than that for PV and **2**. This larger value underscores a greater thermodynamic affinity of citrate, not PV, for complex **2**; thus PV will be displaced by the incoming citrate, providing the kinetic barrier is surmountable at room temperature within a reasonable timescale.

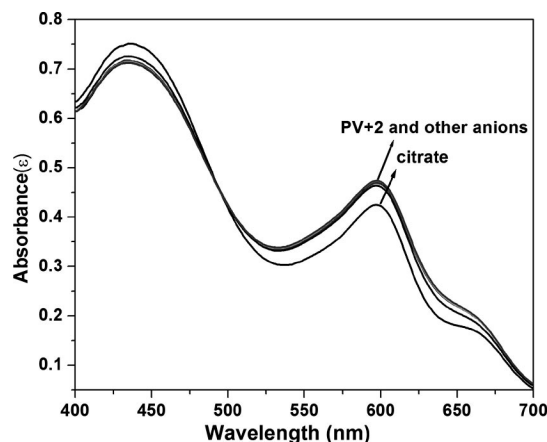


Figure 7. UV/Vis spectrum obtained by addition of different anion solution (250 μM) to a buffered aqueous 1:1 solution of the [PV·**2**] ensemble (50 μM) [10 mM HEPES, pH 7.4].

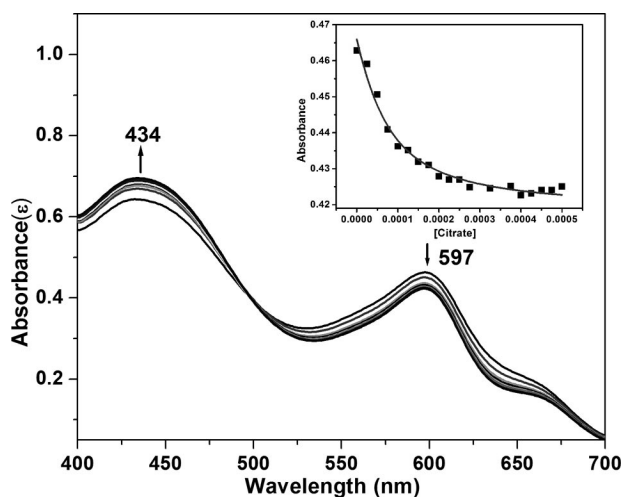
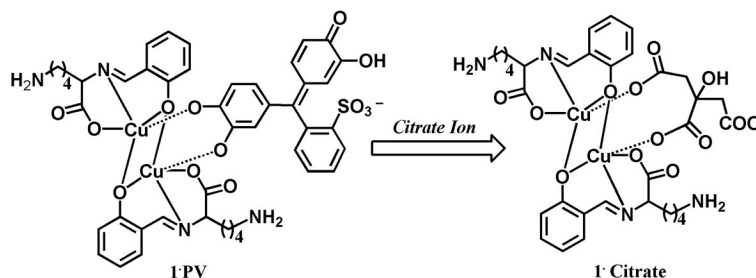


Figure 8. UV/Vis titration spectrum obtained by addition of citrate solution (0–500 μM) to an aqueous buffer solution containing a 1:1 [PV·**2**] ensemble (50 μM) [10 mM HEPES, pH 7.4]. (Inset) Curve fitting of absorbance change vs. [citrate] at 597 nm; $K_a = 1.99 \pm 0.34 \times 10^4 \text{ M}^{-1}$.

This result is generally pertinent to the mechanism of the indicator displacement assay when applied to these useful bimetallic systems; these results will help broaden the use of this mode of detection for important goals such as *chiral analyte* sensing. The citrate ion sensing by these complexes is also reported by colour changes of solutions (e.g., in cuvettes) with the “unaided” eye. In Figure 9, vial 1 contains only the PV indicator, whereas vial 2 contains the blue PV·**2** ensemble. Vials 3–7 contain ensembles with 1 equiv. of different carboxylate anions. Only citrate is able to restore the solution colour of PV, however; other carboxylates do *not* affect the colour of the PV·**2** ensemble. Compound **1** also demonstrates citrate ion selectivity under analogous conditions, but the sensitivity is somewhat better for compound **2** which may turn out to be based in sterics, but is as of yet not precisely clear from the obtained data.



Scheme 3. Proposed mechanism for indicator displacement and possible binding mode of citrate.

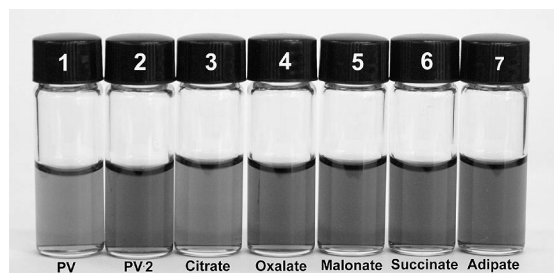


Figure 9. Naked-eye colorimetric detection of citrate ion by indicator displacement in aqueous buffer solution at physiological pH. PV (100 μ M), PV-2 (100 μ M), anions (100 μ M). For a colour version of this Figure, refer to the Supporting Information section.

While our complexes are able to detect the citrate ion selectively, the absorbance changes (Figure 8) are relatively small. The detection change from ca. 0.46 to ca. 0.42 in absorbance is of limited analytical reliability. However this dicopper design serves as an excellent prototype for trials using related systems with different metals, ligation moieties, and cofactors. Further citrate sensing studies will require (i) establishing detection limit, (ii) exploring the dynamic range, (iii) determining reversibility, (iv) analyzing the tolerance to various media and pH values, (v) obtaining binding isotherms for other carboxylates and other potential interfering species, and (vi) possible success of operation in biological media.

We propose the following Scheme 3, based on the cartoon in Scheme 1. Scheme 3 is consistent with Job plot data for this type of system which has been previously tested using PPI in a closely related system.^[14] Direct evidence for the mode of citrate binding (donor atoms) and mechanism of indicator displacement are not supported herein. At this point, we propose a direct O,O' covalent-type interaction. In this solution binding mode, the citrate replaces the *aqua* ligands and interacts with the complex through its two carboxylate sites. However, we cannot rule out that a single carboxylate and alcoholic OH group may be involved.

Conclusions

Two dimeric chiral copper complexes were synthesized by an easy "one-pot" method in which the Schiff base ligands were generated in situ. Both compounds were characterized spectroscopically and structurally. These dimeric complexes are highly soluble and stable in water. The chiral

character of these compounds is confirmed by solution CD spectroscopy in 100% aqueous media. The molecular structures of compounds **1** and **2** possess freely bound axial solvato ligands on the *same side* leading to a C_2 -molecular symmetry. X-ray diffraction data also facilitates an analysis of the magnetic properties of complexes **1** and **2**. Variable-temperature magnetic susceptibility measurements reveal strong antiferromagnetic coupling interactions for both complexes. Due to the dimeric nature of these species in solution, anion sensing was explored in buffered aqueous solutions through the use of indicator displacement assays. Both compounds detect citrate ions over other di- and tricarboxylates in the useful physiological pH region. The sensitivity of compound **2** towards citrate is somewhat enhanced over that of compound **1**. While this sensing is limited, it does exemplify an interesting new design in molecular sensing, when taken together with previous studies of closely related systems.^[14]

Experimental Section

Materials and Physical Measurements: All chemicals used herein were used as received from commercial suppliers (Aldrich and TCI companies). Absorption spectra were measured using a JASCO V-530 UV/Vis spectrophotometer. Solution CD spectra were carried out with a JASCO-815 CD spectropolarimeter in an aqueous HEPES (0.01 M, pH 7.4) buffer solution. Elemental analyses were performed with a EA 110-CHNS-O elemental analyzer. IR spectra were collected in Bruker Equinox 55 spectrometer. The ESI-MS was performed in Bruker micrOTOF II mass spectrometer.

Synthesis of $\text{Na}_2[\text{Cu}(\text{S-lys})_2 \cdot (\text{H}_2\text{O})_2] \cdot (\text{ClO}_4)_2$ (1**):** An aqueous solution of $\text{Cu}(\text{ClO}_4)_2 \cdot 6\text{H}_2\text{O}$ (1.85 g, 5.00 mmol) was added to an ethanolic solution of salicylaldehyde (0.50 mL, 5.00 mmol). The reaction mixture became light green. After 30 min of stirring at room temperature, an aqueous solution of L-lysine (0.73 g, 5.00 mmol) was added dropwise to the reaction mixture, followed by successive slow addition of a portion of aqueous NaOH (0.20 g, 5.00 mmol). A dilute ethanolic solution of Et_3N (0.70 mL, 5.00 mmol) was then added to the reaction mixture which was maintained at a pH of 7–8. The reaction mixture then turned dark bluish green. The stirring was continued for a further 12 h. The reaction mixture was then filtered and kept for evaporation. No solid crystals were observed, so the solvent was evaporated almost to dryness. The reaction mixture was then kept in a vacuum dessicator. After one day, shiny green single crystals suitable for diffraction were obtained from this supernatant liquor; yield 34%. $\text{C}_{52}\text{H}_{72}\text{Cl}_2\text{Cu}_4\text{N}_8\text{Na}_2\text{O}_{24}$ (**1**·2NaClO₄) ($M = 1564.24 \text{ g mol}^{-1}$): calcd. C 39.93, H 4.64, N 7.16; found C 40.14, H 4.76, N 7.15. FTIR (KBr disc): $\tilde{\nu}_{\text{max}} = 3446$,

2927, 1637, 1600, 1448, 1289, 1120 cm^{-1} . MS (ESI): calcd. for $\text{C}_{26}\text{H}_{33}\text{Cu}_2\text{N}_4\text{O}_6$ [$1 - 2\text{H}_2\text{O} + \text{H}^+$] $^+$ 623.1192; found 623.1057.

Synthesis of $[\text{Cu}(\text{S-ornH})_2 \cdot (\text{H}_2\text{O})_2] \cdot (\text{ClO}_4)_2$ (2): Compound **2** was synthesized by exactly the same procedure as **1** was, except with L-ornithine monohydrochloride being substituted for L-lysine; yield 45%. $\text{C}_{24}\text{H}_{34}\text{Cl}_2\text{Cu}_2\text{N}_4\text{O}_{16}$ ($2 \cdot 2\text{ClO}_4$) ($M = 832.53 \text{ g mol}^{-1}$): calcd. C 34.62, H 4.12, N 6.73; found C 34.72, H 4.18, N 6.85. FTIR (KBr disc): $\tilde{\nu}_{\text{max}} = 3466, 1652, 1558, 1486, 1357, 1286 \text{ cm}^{-1}$. MS (ESI): calcd. for $\text{C}_{24}\text{H}_{29}\text{Cu}_2\text{N}_4\text{O}_6$ [$2 - 2\text{H}_2\text{O} + \text{H}^+$] $^+$ 595.0879; found 595.069.

Crystallographic Studies: X-ray diffraction measurements were performed at 293 K with a Bruker SMART 1 K CCD diffractometer using graphite-monochromated Mo- K_α radiation ($\lambda = 0.71073 \text{ \AA}$). Cell parameters were determined and refined by the SMART program.^[21] Data reduction was performed by using SAINT software.^[21] The data were corrected for Lorentz and polarization effects. An empirical absorption correction was applied using the SADABS program.^[22] All intensity data were corrected for Lorentz and polarization effects. The structures were solved by employing direct methods using the SHELXS-97 program^[23] and refined by full-matrix least-squares calculations (F^2) by using the SHELXL-97 software.^[24] All non-H atoms were refined anisotropically against F^2 for all reflections. All hydrogen atoms, except those belonging to the amine nitrogen atom (N2) and the solvent water oxygen atoms, were placed at their calculated positions and refined isotropically. Hydrogen atoms attached to N2 and N4 atoms were located through the use of difference Fourier maps and refined with isotropic displacement coefficients. The ClO_4^- moieties in both compounds were crystallographically disordered. This disorder was elucidated with the aid of the PART command. Crystal data for compounds **1** and **2** are given in Table 1. Selected bond lengths and angles are listed in Table 2.

Table 1. Crystal data collection and refinement data of compounds **1** and **2**.

	1	2
Empirical formula	$\text{C}_{52}\text{H}_{72}\text{Cl}_2\text{Cu}_4\text{N}_8\text{Na}_2\text{O}_{24}$	$\text{C}_{24}\text{H}_{34}\text{Cl}_2\text{Cu}_2\text{N}_4\text{O}_{16}$
FW	1564.24	832.53
T [K]	293(2)	293(2)
Crystal system	monoclinic	monoclinic
Space group	$C2$	$C2$
a [\AA]	17.1571(11)	16.6337(16)
b [\AA]	8.7759(5)	8.8620(9)
c [\AA]	23.3762(14)	11.2159(11)
α [$^\circ$]	90	90
β [$^\circ$]	94.606(4)	92.942(5)
γ [$^\circ$]	90	90
V [\AA^3]	3508.4(4)	1651.1(3)
Z	2	2
$\rho_{\text{calcd.}}$ [Mg m^{-3}]	1.481	1.675
μ [mm^{-1}]	1.362	1.528
$F(000)$	1608	852
Crystal size [mm]	$0.20 \times 0.20 \times 0.10$	$0.3 \times 0.2 \times 0.2$
Reflections collected	19183	20605
Independent reflections	5930 [$R(\text{int}) = 0.0346$]	6275 [$R(\text{int}) = 0.0255$]
Data/restraints/params	5930/40/445	6275/2/235
Absorption correction	empirical	empirical
$T_{\text{max}}, T_{\text{min}}$	0.8758, 0.7724	0.740, 0.704
GOF on F^2	1.088	1.034
$R1^{[a]}, wR2^{[b]}$ [$I > 2\sigma(I)$]	0.0654, 0.1770	0.0301, 0.0785
$R1^{[a]}, wR2^{[b]}$ [all data]	0.0758, 0.1883	0.0388, 0.0928
Flack (x) parameter	0.03(2)	0.037(9)

[a] $R1 = (\Sigma ||F_o| - |F_c||) / \Sigma |F_o|$. [b] $wR2 = [(\Sigma (F_o^2 - F_c^2)^2) / \Sigma w(F_o^2)^2]^{1/2}$.

CCDC-719985 (for **1**) and -719986 (for **2**) contain the supplementary crystallographic data for this paper. These data can be ob-

Table 2. Selected bond lengths and angles for compounds **1** and **2**.

Compound 1			
O(1)–Cu(1)	1.928(4)	O(5)–Cu(2)	1.944(5)
O(1)–Cu(1)#1	1.989(5)	N(1)–Cu(1)	1.921(6)
O(1 W)–Cu(1)	2.367(6)	N(3)–Cu(2)	1.922(6)
O(2 W)–Cu(2)	2.342(6)	Cu(1)–O(1)#1	1.989(5)
O(2)–Cu(1)	1.936(5)	Cu(1)–Cu(1)#1	2.9527(14)
O(4)–Cu(2)	1.927(5)	Cu(2)–O(4)#2	1.974(4)
O(4)–Cu(2)#2	1.974(4)	Cu(2)–Cu(2)#2	2.9689(14)
N(1)–Cu(1)–O(1)	93.5(2)	N(3)–Cu(2)–O(4)	93.7(2)
N(1)–Cu(1)–O(2)	84.0(2)	N(3)–Cu(2)–O(5)	84.3(2)
O(1)–Cu(1)–O(2)	165.4(2)	O(4)–Cu(2)–O(5)	166.3(2)
N(1)–Cu(1)–O(1)#1	166.5(2)	N(3)–Cu(2)–O(4)#2	167.7(2)
O(1)–Cu(1)–O(1)#1	78.2(2)	O(4)–Cu(2)–O(4)#2	77.9(2)
O(2)–Cu(1)–O(1)#1	101.4(2)	O(5)–Cu(2)–O(4)#2	101.8(2)
N(1)–Cu(1)–O(1 W)	99.1(2)	N(3)–Cu(2)–O(2 W)	96.0(2)
O(1)–Cu(1)–O(1 W)	102.6(2)	O(4)–Cu(2)–O(2 W)	99.3(2)
O(2)–Cu(1)–O(1 W)	92.0(2)	O(5)–Cu(2)–O(2 W)	94.4(2)
O(1)#1–Cu(1)–O(1 W)	93.2(2)	O(4)#2–Cu(2)–O(2 W)	94.2(2)
Symmetry transformations: #1 $-x, y, -z$ #2 $-x + 2, y, -z + 1$			
Compound 2			
Cu(1)–N(1)	1.9307(15)	Cu(1)–O(1)#1	1.9781(12)
Cu(1)–O(1)	1.9341(13)	Cu(1)–O(1 W)	2.297(2)
Cu(1)–O(2)	1.9340(14)	Cu(1)–Cu(1)#1	2.9641(4)
N(1)–Cu(1)–O(1)	93.76(6)	O(2)–Cu(1)–O(1)#1	100.16(6)
N(1)–Cu(1)–O(2)	84.66(6)	N(1)–Cu(1)–O(1 W)	98.07(7)
O(1)–Cu(1)–O(2)	162.69(7)	O(1)–Cu(1)–O(1 W)	99.25(7)
N(1)–Cu(1)–O(1)#1	168.83(6)	O(2)–Cu(1)–O(1 W)	98.04(8)
O(1)–Cu(1)–O(1)#1	78.62(6)	O(1)#1–Cu(1)–O(1 W)	91.26(7)
Symmetry transformations: #1 $-x + 1, y, -z + 1$ #2 $-x + 1, y, -z + 2$			

tained free of charge from The Cambridge Crystallographic Data Centre via www.ccdc.cam.ac.uk/data_request/cif.

Supporting Information (see also the footnote on the first page of this article): All types of UV/Vis spectra related to this work, Job plots, fitting diagrams, and Figure S11 (Scheme 2, designed in colour), Figure S12 (Figure 9, designed in colour).

Acknowledgments

D. G. C. acknowledges support from Korea Science and Engineering Foundation (KOSEF) (grant no. R01-2008-000-12388-0). S. K. is grateful to the Ministry of Education, Science & Technology for a Brain Korea 21 (BK 21) postdoctoral fellowship, and to the laboratory of Prof. Hyotcherl Ihlee of the Korea Advanced Institute of Science & Technology (KAIST) for a portion of recent additional financial support. The authors acknowledge the Korea Basic Science Institute (KBSI) for obtaining variable-temperature magnetic susceptibility measurements.

- [1] a) A. D. Garnovskii, A. P. Sadimenko, M. I. Sadimenko, D. A. Garnovskii, *Coord. Chem. Rev.* **1998**, *173*, 31; b) S. Yamada, *Coord. Chem. Rev.* **1999**, *190–192*, 537–555; c) R. L. Lieberman, A. C. Rosenzweig, *Nature* **2005**, *434*, 177–182.
- [2] a) C.-M. Che, H.-L. Kwong, W.-C. Chu, K.-F. Cheng, W.-S. Lee, H.-S. Yu, C.-T. Yeung, K.-K. Cheung, *Eur. J. Inorg. Chem.* **2002**, *6*, 1456–1463; b) R. Ferreira, C. Freire, B. de Castro, A. P. Carvalho, J. Pires, M. B. de Carvalho, *Eur. J. Inorg. Chem.* **2002**, *11*, 3032–3038; c) A. Burkhardt, A. Buchholz, H. Goerls, W. Plass, *Eur. J. Inorg. Chem.* **2006**, *17*, 3400–3406; d) Y.-B. Jiang, H.-Z. Kou, R.-J. Wang, A.-L. Cui, *Eur. J. Inorg. Chem.* **2004**, 4608–4615; e) S. Thakurta, P. Roy, G. Rosair, C. J. Gómez-García, E. Garribba, S. Mitra, *Polyhedron* **2009**, *28*, 695–702; f) F. Tuna, L. Patron, Y. Journaux, M. Andruh, W. Plass, J.-C. Trombe, *J. Chem. Soc., Dalton Trans.* **1999**, 539–546; g) H.-Y. Chao, D. G. Churchill, *J. Chem. Educ.* **2008**, *85*, 1210–1214.
- [3] a) E. M. Hodnett, P. D. Mooney, *J. Med. Chem.* **1970**, *13*, 786; b) C. A. Bolos, G. St. Nikolov, L. Ekateriniadou, A. Kortsaris, D. A. Kyriakidis, *Met.-Based Drugs* **1998**, *5*, 323–332; c) G. Plesch, C. Friebel, O. Svajlenova, J. Krättsmar-Smogrovic, D. Mlynarcik, *Inorg. Chim. Acta* **1988**, *139*, 151; d) G. Cerchiaro, K. Aquilano, G. Filomeni, G. Rotilio, M. R. Ciriolo, A. M. D. C. Ferreira, *J. Inorg. Biochem.* **2005**, *99*, 1433–1450; e) G. Filomeni, G. Cerchiaro, A. M. D. C. Ferreira, J. Z. Pedersen, A. De Martino, G. Rotilio, M. R. Ciriolo, *J. Biol. Chem.* **2007**, *282*, 12010–12021; f) A. T. Chaviara, E. E. Kioseoglou, A. A. Pantazaki, A. C. Tshipis, P. A. Karipidis, D. A. Kyriakidis, C. A. Bolos, *J. Inorg. Biochem.* **2008**, *102*, 1749–1764; g) V. C. da Silveira, J. S. Luz, C. C. Oliveira, I. Graziani, M. R. Ciriolo, A. M. D. C. Ferreira, *J. Inorg. Biochem.* **2008**, *102*, 1090–1103; h) P. A. N. Reddy, M. Nethaji, A. R. Chakravarty, *Eur. J. Inorg. Chem.* **2004**, *7*, 1440–1446.
- [4] a) V. G. Gibson, S. K. Spitzmesser, *Chem. Rev.* **2003**, *103*, 283–316; b) S. Yamada, *Coord. Chem. Rev.* **1999**, *190–192*, 537–555; c) H.-B. Zhu, Z.-Y. Dai, W. Huang, K. Cui, S.-H. Gou, C.-J. Zhu, *Polyhedron* **2004**, *23*, 1131–1137; d) A. G. Dosseter, T. F. Jamison, E. N. Jacobsen, *Angew. Chem. Int. Ed.* **1999**, *38*, 2398–2400; e) V. B. Sharma, S. L. Jain, B. Sain, *J. Mol. Catal. A* **2004**, *219*, 61–64; f) J. F. Folmer-Andersen, V. M. Lynch, E. V. Anslyn, *J. Am. Chem. Soc.* **2005**, *127*, 7986–7987.
- [5] a) X. Yang, J. D. Ranford, J. J. Vittal, *Cryst. Growth Des.* **2004**, *4*, 781–788; b) M. A. Alam, R. R. Koner, A. Das, M. Nethaji, M. Ray, *Cryst. Growth Des.* **2007**, *7*, 1818–1824.
- [6] For reviews of anion sensing, see: a) M. H. Filby, J. W. Steed, *Coord. Chem. Rev.* **2006**, *250*, 3200–3218; b) R. Martinez-Manez, F. Sancenon, *Coord. Chem. Rev.* **2006**, *250*, 3081–3093; c) A. P. Davis, *Coord. Chem. Rev.* **2006**, *250*, 2939–2951; d) R. Martinez-Manez, F. Sancenon, *Chem. Rev.* **2003**, *103*, 4419–4476; e) P. D. Beer, J. Cadman, *Coord. Chem. Rev.* **2000**, *205*, 131–155.
- [7] a) S. L. Wiskur, H. Ait-Haddou, J. J. Lavigne, E. V. Anslyn, *Acc. Chem. Res.* **2001**, *34*, 963–972; b) L. Fabbri, M. Licchelli, A. Taglietti, *Dalton Trans.* **2003**, 3471–3479; c) J. Zhao, T. D. James, *Chem. Commun.* **2005**, 1889–1891; d) R. Martinez-Manez, F. Sancenon, *J. Fluoresc.* **2005**, *15*, 267–285; e) K. Ghosh, G. Masanta, *Tetrahedron Lett.* **2006**, *47*, 2365–2369.
- [8] T. N. Popova, M. A. A. Pinheiro de Carvalho, *Biochim. Biophys. Acta* **1998**, *1364*, 307–325.
- [9] D. P. Simpson, *Am. J. Physiol.* **1983**, *244*, F223–F234.
- [10] a) C. Schmuck, M. Schwegmann, *J. Am. Chem. Soc.* **2005**, *127*, 3373–3379; b) C. Schmuck, M. Schwegmann, *Org. Biomol. Chem.* **2006**, *4*, 836–838; c) D. Parker, J. Yu, *Chem. Commun.* **2005**, 3141–3143; d) K. Ghosh, T. Sen, R. Fröhlich, *Tetrahedron Lett.* **2007**, *48*, 2935–2938; e) A. L. Koner, J. Schatz, W. M. Nau, U. Pischel, *J. Org. Chem.* **2007**, *72*, 3889–3895; f) A. Metzger, V. M. Lynch, E. V. Anslyn, *Angew. Chem. Int. Ed. Engl.* **1997**, *36*, 862–865; g) A. Metzger, E. V. Anslyn, *Angew. Chem. Int. Ed.* **1998**, *37*, 649–652; h) J. J. Lavigne, E. V. Anslyn, *Angew. Chem. Int. Ed.* **1999**, *38*, 3666–3669; i) L. Fabbri, F. Foti, A. Taglietti, *Org. Lett.* **2005**, *7*, 2603–2606; j) M. I. Burguete, F. Galindo, S. V. Luis, L. Vigara, *Dalton Trans.* **2007**, 4027–4033; k) M. P. Clares, C. Lodeiro, D. Fernandez, A. J. Parola, F. Pina, E. Garcia-Espana, C. Soriano, R. Tejero, *Chem. Commun.* **2006**, 3824–3826; l) M. Comes, G. Rodríguez-López, M. D. Marcos, R. Martínez-Mañez, F. Sancenón, J. Soto, L. A. Villaescusa, P. Amorós, D. Beltrán, *Angew. Chem. Int. Ed.* **2005**, *44*, 2918–2922; m) L. A. Cabell, M. D. Best, J. J. Lavigne, S. E. Schneider, D. M. Perreault, M. K. Monahan, E. V. Anslyn, *J. Chem. Soc. Perkin Trans. 2* **2001**, 315–323.
- [11] a) A. Kazemzadeh, F. Moztafzadeh, *Sens. Actuators, B* **2005**, *106*, 832–836; b) L. Tang, J. Park, H.-J. Kim, Y. Kim, S. J. Kim, J. Chin, K. M. Kim, *J. Am. Chem. Soc.* **2008**, *130*, 12606–12607; c) M. Boiocchi, M. Bonizzoni, L. Fabbri, G. Piovani, A. Taglietti, *Angew. Chem. Int. Ed.* **2004**, *43*, 3847–3852; d) A. M. Costero, M. Colera, P. Gavina, S. Gil, U. Llaosa, *Tetrahedron* **2008**, *64*, 7252–7257; e) K. Ghosh, G. Masanta, *Tetrahedron Lett.* **2008**, *49*, 2592–2597; f) Y.-P. Yen, K.-W. Ho, *Tetrahedron Lett.* **2006**, *47*, 1193–1196.
- [12] The use of a Schiff base species as a sensor; a) D. Ray, P. K. Bharadwaj, *Inorg. Chem.* **2008**, *47*, 2252–2254; b) P. Roy, K. Dhara, M. Manassero, J. Ratha, P. Banerjee, *Inorg. Chem.* **2007**, *46*, 6405–6412; c) K. Dhara, K. Sarkar, P. Roy, M. Nandi, A. Bhaumik, P. Banerjee, *Tetrahedron* **2008**, *64*, 3153–3159; d) D. Saravanakumar, S. Devaraj, S. Iyyampillai, K. Mohandossb, M. Kandaswamy, *Tetrahedron Lett.* **2008**, *49*, 127–132.
- [13] a) L. Fabbri, N. Marcotte, F. Stomeo, A. Taglietti, *Angew. Chem. Int. Ed.* **2002**, *41*, 3811–3814; b) J. F. Folmer-Andersen, V. M. Lynch, E. V. Anslyn, *Chem. Eur. J.* **2005**, *11*, 5319–5326.
- [14] a) S. Khatua, S. H. Choi, J. Lee, K. Kim, Y. Do, D. G. Churchill, *Inorg. Chem.* **2009**, *48*, 2993–2999; b) S. Khatua, S. H. Choi, J. Lee, J. O. Huh, Y. Do, D. G. Churchill, *Inorg. Chem.* **2009**, *48*, 1799–1801. For a description of common chemical explosion hazards including perchlorates and closely related species, see: c) D. G. Churchill, *J. Chem. Educ.* **2006**, *83*, 1798.
- [15] a) C.-T. Yang, M. Vetrichelvan, X. Yang, B. Moubarak, K. S. Murray, J. J. Vittal, *Dalton Trans.* **2004**, 113–121; b) X. Wang, J. Ding, J. J. Vittal, *Inorg. Chim. Acta* **2006**, *359*, 3481–3490; c) S. M. Couchman, J. C. Jeffery, P. Thornton, M. D. Ward, *J. Chem. Soc., Dalton Trans.* **1998**, 1163–1169; d) V. K. Muppidi, S. Pal, *Eur. J. Inorg. Chem.* **2006**, *14*, 2871–2877.
- [16] a) L. Rodriguez, E. Labisbal, A. Sousa-Pedrares, J. A. Garcia-Vazquez, J. Romero, M. L. Duran, J. A. Real, A. Sousa, *Inorg. Chem.* **2006**, *45*, 7903–7914; b) B. Sreenivasulu, F. Zhao, S. Gao, J. J. Vittal, *Eur. J. Inorg. Chem.* **2006**, *13*, 2656–2670.

- [17] W. H. Crawford, H. W. Richardson, J. R. Wasson, D. J. Hodgson, W. E. Hatfield, *Inorg. Chem.* **1976**, *15*, 2107–2110.
- [18] a) A. P. de Silva, H. Q. N. Gunaratne, T. Gunnlaugsson, A. J. M. Huxley, C. P. McCoy, J. T. Rademacher, T. E. Rice, *Chem. Rev.* **1997**, *97*, 1515–1566; b) F. P. Schmidtchen, M. Berger, *Chem. Rev.* **1997**, *97*, 1609–1646.
- [19] a) K. Niikura, A. Metzger, E. V. Anslyn, *J. Am. Chem. Soc.* **1998**, *120*, 8533–8534; b) S. L. Wiskur, H. A. Haddou, J. J. Lavigne, E. V. Anslyn, *Acc. Chem. Res.* **2001**, *34*, 963–972; c) B. T. Nguyen, E. V. Anslyn, *Coord. Chem. Rev.* **2006**, *250*, 3118–3127; d) L. Fabbri, M. Licchelli, A. Taglietti, *Dalton Trans.* **2003**, 3471–3479; e) D. J. Oh, K. H. Ahn, *Org. Lett.* **2008**, *10*, 3539; f) M. S. Han, D. H. Kim, *Angew. Chem. Int. Ed.* **2002**, *41*, 3809; g) L. Zhu, Z. Zhong, E. V. Anslyn, *J. Am. Chem. Soc.* **2005**, *127*, 4260–4269; h) J. F. Folmer-Andersen, V. M. Lynch, E. V. Anslyn, *Chem. Eur. J.* **2005**, *11*, 5319–5326.
- [20] a) A. K. Connors, *Binding Constants*, Wiley, New York, **1987**; b) B. Valeur, J. Pouget, J. Bourson, M. Kaschke, N. P. Ernsting, *J. Phys. Chem.* **1992**, *96*, 6545.
- [21] *SMART* and *SAINT*, Area Detector Software Package and SAX Area Detector Integration Program, Bruker Analytical X-ray, Madison, WI, **1997**.
- [22] *SADABS*, Area Detector Absorption Correction Program, Bruker Analytical X-ray, Madison, WI, **1997**.
- [23] G. M. Sheldrick, *SHELXS-97: Program for Crystal Structure Determination*, *Acta Crystallogr., Sect. A* **1990**, *46*, 467–473.
- [24] a) G. M. Sheldrick, **1999**, *SHELXL-97: Program for Crystal Structure Solution and Refinements*, University of Göttingen, Göttingen, Germany; b) G. M. Sheldrick, *Acta Crystallogr., Sect. A* **2008**, *64*, 112–122.

Received: April 20, 2009

Published Online: June 25, 2009